

Numerical Simulation of Periodical Turbulent Shear Vortexes in a Submerged Water Jet

Guoyi Peng¹⁺, Hideto Ito¹ and Shimizu Sheiji¹

¹College of Engineering, Nihon University

Abstract: With the purpose of improving the performance of water jet devices numerical analysis of water jets issuing from a submerged nozzle is carried out by applying a two-phase mixture flow method. Unsteady flow of water jet accompanied by cavitation is calculated by solving a set of Reynolds Averaged Navier-Stokes equations and the intensity of cavitation is evaluated by the gas volume fraction based on an estimation of average bubble radius varying with the local pressure. Cavitating and no-cavitation water jets are treated under different cavitation numbers. The results demonstrate that a ring-like starting vortex is generated at the head of impulsively injected jet and a low-pressure region is formed at the center of the ring-like vortex. With developing of submerged jet shear vortexes are generated sequentially on the jet periphery and a sequence of shear vortexes shade downstream periodically. Under the effect of shear vortexes pressure varies alternatively on the jet periphery and thus cavitation takes place sequentially in the low-pressure area of vortex cores once the cavitation number is decreased to a critical value.

Keywords: Submerged water jet, unsteady flow, turbulence, cavitation, numerical simulation

1. Introduction

High-speed jets of water have been utilized in many fields such as cleaning of complicated mechanical products, cutting of solid materials etc. As a useful technology of cavitation utilization, the high-speed jet of water into water, which is usually called submerged water jet, has been attracting much attention especially. Experimental investigations demonstrated that impacts caused by the collapse of cavitation bubbles play an important role in effects of the submerged water jet and unsteady cavitation is advantageous to enhance machining abilities of the submerged water jet [1-3]. Therefore, intensification of cavitation impacts comes to be a real requirement with expanding applications of the submerged water jet. Although some experimental studies such as visualization of cavitating jets have been made [4], the structure of cavitating vortexes in submerged water jet and the behaviour of unsteady cavitation bubbles are still unclear because of difficulty for observing directly the interior of flows with numerous micro bubbles.

On the other hand, much attention has been paid to numerical analyses of cavitating flows and considerable effort has been made in modelling of cavitation phenomena [5, 6]. Due to the growth and collapse of cavitation bubbles, near fields of bubbles reveal to be compressible, while far-fields full of liquid fluid are essentially incompressible. Both the compressible and incompressible features, therefore, coexist in cavitating flows [7]. For the difficulty in taking account of all the above features, numerical computations of cavitating flow have been conventionally carried out under various simplifications such as low-speed, potential, and incompressible flows. So far, cavitating flows encountered in engineering practice are treated mainly by two different approaches of two-fluid method and two-phase mixture flow method. The two-fluid method takes account of the velocity slip between the liquid and gas phases by computing the flows of working liquid and cavitation bubbles one by one. This method is rational but the computed flow fields

⁺Corresponding author. Tel.: +81-249568766.
E-mail address: peng@mech.ce.nihon-u.ac.jp.

strongly depend upon the physical models used for evaluating the interactions of liquid and bubbles [8, 9]. The so-called two-phase mixture flow method ignores the velocity slip between the liquid and gas phases by assuming that the gas phase disperses in the form of small bubbles and flows at the same velocity together with the liquid phase [10, 11]. In most engineering practice cavitation takes place in low-pressure regions of relatively high velocity where the velocity slip between the liquid and the gas phases is rather small and the simplification is fairly acceptable. Thus, the equal-velocity method has been widely applied in cavitating flow computations by combined with certain cavitation models.

Focused on the vortex structure of submerged water jets this paper presents a two-phase mixture flow method by combining an unsteady turbulent flow computation and a simplified estimation of bubble cavitation. Unsteady flow of bubble-liquid two-phase mixture are computed by solving a set of RANS equations and the intensity of cavitation is evaluated by the gas volume fraction based on an estimation of average bubble radius in local field. Both cavitating and non-cavitating water jets are treated under different cavitation numbers. The structure of shear vortices caused in submerged water jet and the behavior of cavitating bubbles are investigated.

2. Flow Governing Equations and Numerical Approach

2.1. Governing equations for the flow of homogeneous cavitation mixture

Concerning flows of the fluid mixture, cavitation usually takes place in low-pressure regions of relative high velocity and the size of cavitation bubbles is very small compared to its flow field. So, bubbles and the working liquid can be sufficiently well mixed and their relative motion in a small local area may be neglected. The fluid mixture of liquid and cavitation bubbles is then treated as a two-phase fluid medium. The mean density and the mean viscosity of two-phase mixture are given as follows.

$$\rho = \rho_L(1 - \alpha) + \rho_G\alpha \quad (1)$$

$$\mu = (1 - \alpha)(1 + 2.5\alpha)\mu_L + \alpha\mu_G \quad (2)$$

where ρ denotes fluid density and μ does the viscosity. α denotes the volume fraction of gas phase included in the fluid mixture, and subscripts L and G do the liquid and the gas phase, respectively. With regard to the flow computation of such a two-phase mixture Reynolds Averaged Navier-Stokes equations (RANS) for variable fluid density are employed. Assuming that the variation of temperature caused by cavitation is negligible we may remove the energy equation from a set of flow governing equations. Thus, equations of mass and momentum conservation are given as follows.

$$\frac{\partial \rho}{\partial t} + \nabla \cdot (\rho \mathbf{u}) = 0 \quad (3)$$

$$\frac{\partial}{\partial t}(\rho \mathbf{u}) + \nabla \cdot (\rho \mathbf{u} \mathbf{u} - \boldsymbol{\tau}) = -\nabla p + \mathbf{g} \quad (4)$$

where \mathbf{u} denotes the velocity vector, p the local pressure, and \mathbf{g} the gravity. $\boldsymbol{\tau}$ does the stress tensor and its components are given in tensor form as follows.

$$\tau_{ij} = 2\mu S_{ij} - \frac{2}{3}\mu(\nabla \cdot \mathbf{u})\delta_{ij} - \overline{\rho u_i' u_j'} \quad (5)$$

where i and j ($=1, 2, 3$) denote respectively three components of the coordinates. δ_{ij} denotes the Kronecker delta, S_{ij} the strain tensor, and $-\overline{\rho u_i' u_j'}$ the Reynolds stress which is related to the mean velocity field. In order to evaluate the effect of flow turbulence the RNG k - ε model [12] for high Reynolds number flow is adopted and the Reynolds stress tensor is then given as follows.

$$-\overline{\rho u_i' u_j'} = 2\mu_t S_{ij} - \frac{2}{3}(\mu_t \nabla \cdot \mathbf{u} + \rho k)\delta_{ij} \quad (6)$$

where μ_t denotes the eddy viscosity, which is defined as following by the turbulence energy k and the turbulence dissipation rate ε .

$$\mu_t = \rho C_\mu k^2 / \varepsilon \quad (7)$$

k and ε are then solved by their transportation equations given in the references [13].

2.2. Estimation of cavitation

As mentioned above the fluid mixture of liquid and cavitation bubbles is treated as a gas-liquid two-phase fluid medium, and the gas phase is further supposed to disperse in the liquid phase in the form of micro bubbles. According to the size and the number density of bubbles the gas volume fraction of the two-phase mixture is then given by the following formula.

$$\alpha = \frac{4}{3} \pi n_b R_b^3 \quad (8)$$

where R_b denotes the average bubble radius in a local area and n_b does the mean number density of micro bubbles. In the most engineering situations there are plenty of nuclei in the working liquid for the inception of cavitation. Thus, the bubble number density n_b is taken to be constant by neglecting its slight variation and our primary focus is put on proper account of bubble growth and collapse. For estimation of bubble size it is assumed that cavitation takes place when a local static pressure falls below a critical one, which is taken to be the saturation pressure of the liquid. Based on the theory of bubble dynamics the radius R_b of cavitation bubbles in a local field is calculated by the following simplified Rayleigh-Plesset equation [14].

$$R_b \frac{D^2 R_b}{Dt^2} + \frac{3}{2} \left(\frac{DR_b}{Dt} \right)^2 = \frac{p_v - p}{\rho_L} \quad (9)$$

where $D/Dt = \partial/\partial t + u_i \partial/\partial x_i$, denotes the Lagrangian differential operator and p_v does the saturation vapour pressure. As an initial problem the above equation is solved under given initial condition of that $R_b(x, t) = R_0$ and $DR_b/Dt = 0$ when $t = 0$.

2.3. Discretization and pressure-based computational algorithm

Equations (3) (4) and (9) constitutes a set of equations for unsteady turbulent cavitating flow. These equations are discretized by the finite volume method except that Eq (9) for the bubble radius is solved by the second-order Runge-Kutta method. Computation domain is divided into quadrilaterals and all flow variables are defined at the centre of cells by collocated arrangement. The temporal term is discretized by an implicit Crank-Nicolson scheme with second-order accuracy in time. The Spatial diffusion terms are approximated by cell face-centred expressions defined with nodal values and convective fluxes are discretized by the central difference scheme. Algebraic equations obtained through discretization of flow governing equations are solved by the PISO algorithm of multiple predictor-correctors [15]. The criterion of convergence is given to be that the relative error is smaller than 1.0×10^{-3} for pressure and 5.0×10^{-3} for velocity. Other scalar variables are then calculated from the flow field at present time step.

3. Computational Results and Discussions

Figure 1 shows the schematic diagram of submerged water jet concerned, where a jet of water is issued from a pipe nozzle into a cylindrical tank full of still water. The device is set vertically and the gravity works in the reverse direction of axial coordinate. By focusing our concentration on the structure of shear vortices before they break down, the assumption of axisymmetric flow is adopted here. As shown in the figure, a right-hand cylindrical coordinates denoted by (r, θ, z) is adopted and the origin is taken at the centre of nozzle exit. The computation domain consists of the interior of cylindrical reservoir tank as well as a part of the nozzle interior taken to be $-5d \leq z \leq 0$ and $0 \leq r \leq 0.5d$, where d denotes the nozzle diameter.

Boundary conditions for flow computation are given as follows. At the nozzle inlet ($z = -5d$, $0 \leq r < 0.5d$), a velocity condition is given by $u_z = u_{in}$ and $u_r = u_\theta = 0$. The profile of u_{in} is nearly uniform in high Reynolds flow as the present case since the viscous boundary layer on the inner wall is very thin. The turbulence kinetic energy k_{in} and the turbulence dissipation rate ε_{in} are respectively defined by $k_{in} = 0.03 u_{in}^2$ and $\varepsilon_{in} = C_\mu k_{in}^{3/2} / l_{in}$, where l_{in} is the turbulent scale given by $l_{in} = 0.015d$. At the outlet

boundary, a pressure condition $p = p_0$ is imposed, and the gradients of velocity components and other scalar variables are given to be zero. At the z -axis, the Neumann condition is imposed. On the wall boundaries the non-slip condition of viscous flow is applied in consideration of boundary layer effects. To save computation cost, the wall function method is adopted and a non-slip velocity distribution is defined near the wall boundary according to the law of wall for turbulent boundary layer. So, the need to use much fine grids inside boundary layer is avoided.

The jet is started to inject into reservoir tank under a certain working pressure. Considering the acceleration property of jet system a time dependent injection velocity is specified as $u_m = u_0 \min(1, t/t_0)$, where u_0 denotes a constant velocity and t_0 is the acceleration time of jet system. For normalization of unsteady flow property, a dimensionless vortex formation time is defined as $t^* = u_0 t / d$ [16]. As a discriminant of cavitations a device cavitation number is defined as follows.

$$\sigma_i = \frac{p_o - p_v}{\rho_0 u_0^2 / 2} \quad (10)$$

where ρ_0 denotes the density of water, p_o the discharge pressure and p_v the saturated vapor pressure.

3.1. Formation and development of ring-link starting vortex

Flows of submerged water jet impulsively started are simulated under different cavitation number by adjusting the injection velocity and the discharge pressure. Figure 2 shows, as an example, the flow structure of no-cavitating submerged jet at the instant when $t^* = 13$ ($u_0 = 20$ m/s, $\sigma_i = 0.99$). Figure 2 (a) presents the distribution of shear vortices where the red colour denotes the liquid jet newly injected and the blue one does the liquid filled in the reservoir tank. Figure 2 (b) and (c) respectively do the maps of isobars and velocity vectors at the given condition, in which the vortex A is called to be ring-like starting vortex and B and C are two shear vortices generated on the jet periphery just behind the starting vortex. It is confirmed that the standoff distance of ring-like starting vortex increases approximately linearly with the vortex formation time under different injection velocities [16, 17]. Comparing Fig. 2 (a) (b) and (c) we understand that static pressure drops in the centre of shear vortices located periodically on the jet periphery. As the ring-like starting vortex flows downstream pressure on the jet periphery varies alternatively along the flow direction. But the pressure at the centre of starting vortex drops greatly and a very low pressure region denoted by blue colour is formed. The result implies that cavitation inception should take place initially in the starting vortex once the cavitation number is decreased to a critical value. This has been confirmed by experimental observations of cavitating submerged jet [18].

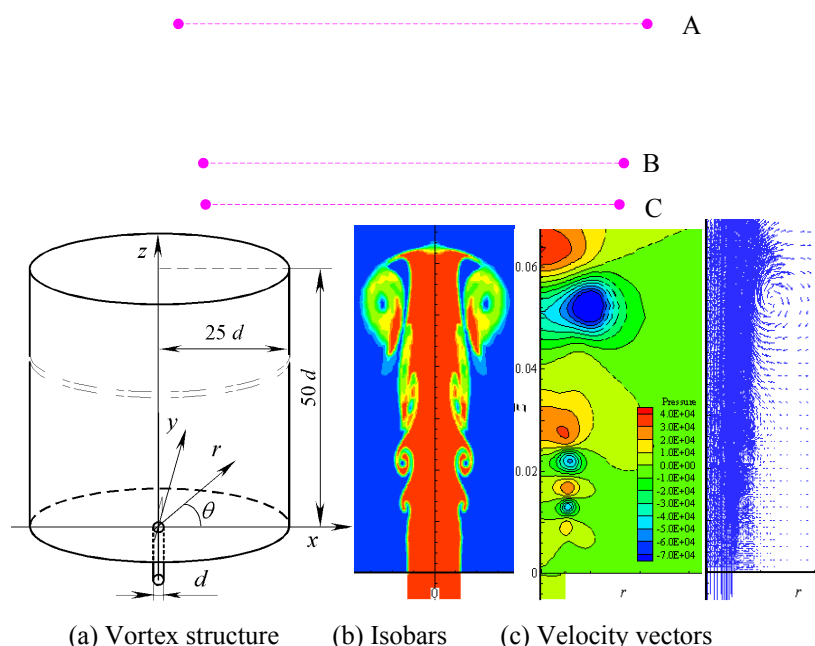


Fig. 1: Scheme of submerged water jet Fig. 2: Ring-like starting vortex generated in submerged jet

3.2. Behavior of shear vortices

Concerning the behavior of shear vortices generated on the jet periphery the structure of unsteady submerged jet are investigated from a series of computational results. Figure 3 shows the instantaneous distribution of shear vortices generated in non-cavitating jet ($\sigma_i = 0.99$ and $u_0 = 20$ m/s) in a time sequence. Figure 4 (a) to (g) respectively present contour maps of fluid volume fraction extracted from a sequence of results in a certain time interval, where the red colour denotes the liquid jet injected and the blue one does the liquid in the tank. As shown in the figure shearing vortices denoted by A, B, and C are generated sequentially on the jet periphery grow into bigger ones while shade downstream. When the small vortex A develops to a certain extent another small vortex denoted by D is generated newly as shown in Fig. 3 (g). According to the result we understand that a sequence of shear vortices is generated around the jet periphery and shades downstream periodically at the stable state of well-developed submerged jet. Under the effect of shear vortices pressure on the shear layer varies alternatively and thus cavitation may take place periodically around the jet periphery when the low pressure decreases to the vapour pressure.

Figure 4 shows the distributions of velocity vector and correspond contour maps of gas volume fraction at different instants when the cavitation number σ_i is decreased to 0.12 ($u_0 = 20$ m/s, $p_0 = 0.25p_a$). Here, the blue color indicates the liquid phase and the red one does the vapor phase, and the closed areas formed by contours of VOF ($f = 1 - \alpha \leq 0.9$) are considered to be cavitation region containing a mass of cavitation bubbles. Figure 4 (a) presents the distribution of velocity vectors and contour map of VOF when the ring-like starting vortex flows far downstream and Fig. 4 (b) does the distribution of cavitating jet at a well-developed stage. The figures demonstrate that cavitation bubbles are generated continually in the low pressure area of shear vortex cores on the shear layer and shades downstream periodically along the jet periphery. This may be the reason that bubble cloud generated in cavitating submerged water jets is often observed to eject downstream periodically in visualization experiments [4, 18].

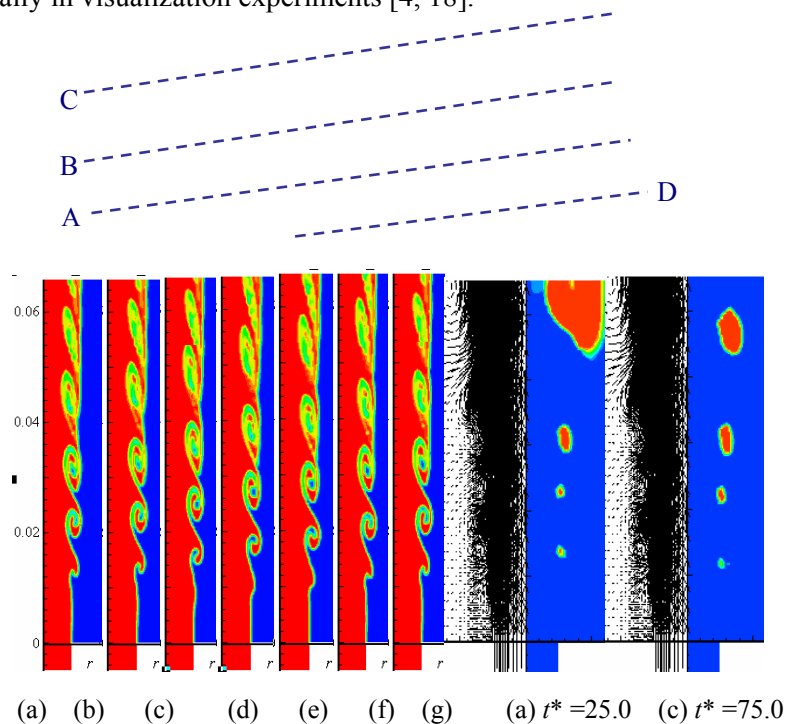


Fig. 3: Instantaneous shear vortices generated in a no-cavitating jet ($u_0=20$ m/s, $\sigma_i = 0.99$)

Fig. 4: Instantaneous distribution of bubble cavities in a cavitating jet ($u_0=20$ m/s, $\sigma_i = 0.12$)

4. Conclusions

A two-phase mixture flow method has been developed by combining a turbulent two-phase flow computation and a simplified estimation of bubble cavitation and applied to the case of water jets injected impulsively from a submerged nozzle. Both non-cavitating and cavitating flows of submerged water jets are investigated and the results demonstrate that:

(1) With impulsive injection of submerged jet a ring-like starting vortex is generated at the head of jet and a low pressure region is formed at the centre of the ring-like vortex, where cavitation is easy to take place under a low cavitation number.

(2) At the stable stage of well-developed jet, shear vortices are generated sequentially on the jet periphery near to the nozzle exit and a sequence of shear vortices shed downstream periodically. Under the effect of shear vortices pressure varies alternatively on the shear layer. So, cavitation takes place consequentially in the low-pressure area of vortex cores when the cavitation number is lower enough.

5. Acknowledgements

This work has been supported by JSPS, Grant-in-Aid for Scientific Research(C) (N0. 22560177).

6. References

- [1] K.K. Ooi. Scale Effects on Cavitation Inception in Submerged Water Jets: A New Look. *J. Fluid Mech.*, 1985, **151**, 367-390.
- [2] T.J. O'Hern. An Experimental Investigation of Turbulent Shear Flow Cavitation. *J. Fluid Mech.*, 1990, **215**, 365-391.
- [3] A. Yamaguchi and S. Shimizu. Erosion due to Impingement of Cavitation Jet. *J. Fluid Eng.*, 1987, **109**, 442-447.
- [4] H. Ito et al. Observation of Cavitating Jets Issuing from a Sheathed Nozzle. In: S. Shimizu and G. Peng (eds.), *Water Jetting Technology for LOHAS*, International Academic Printing Co. Ltd., Tokyo, 2009, 97-100.
- [5] Kubota, et al. New Modeling of Cavitating Flow: A Numerical Study of Unsteady Cavitation on a Hydrofoil Section. *J. Fluid Mech.*, 1992, **240**, 59-96.
- [6] K. Singhal, et al. Mathematical Basis and Validation of the Full Cavitation Model. *J. Fluids Eng.*, 2002, **124**, 617-624.
- [7] G. Peng, et al., An Improved CIP-CUP Method for Submerged Water Jet Flow Simulation. *JSME Int. J. (B)*, 2001, **44**, 497-504.
- [8] Y. Delannoy and J. Kueny. Two Phase Flow Approach in Unsteady Cavitation Modeling, *Cavitation and Multiphase Flow Forum*, ASME FED-Vol.98, 1990, 153-158.
- [9] R. Egashira, T. Yano and S. Fujikawa. Linear Wave Propagation of Fast and Slow Modes in Mixtures of Liquid and Gas Bubbles. *Fluid Dynamic Research*, 2004, **34**, 317-334.
- [10] I. Senocak and W. Shyy. A Pressure-Based Method for Turbulent Cavitating Flow Computations, *J. Comput. Phys.*, 2002, **176**, 363-383.
- [11] Y. Iga et al. Numerical Study of Sheet Cavitation Breakoff Phenomenon on a Cascade Hydrofoil. *J. Fluids Eng.*, 2003, **125**, 643-651.
- [12] V. Yakhot, et al. Development of Turbulence Models for Shear Flows by a Double Expansion Technique. *Phys. Fluids*, 1992, **A4(7)**, 1510-1520.
- [13] D. Wilcox. *Turbulence Modeling for CFD*. DCW Industries, 2nd ed. 2002, 540.
- [14] E. Brennen. *Cavitation and Bubble Dynamics*. Oxford Univ. Press, 1995, 304.
- [15] R.I. Issa. Solution of the Implicitly Discretised Fluid Flow Equations by operator-splitting, *J. Comp. Phys.*, 1986, **62**, 40-65.
- [16] M. Gharib, et al. Universal Time Scale for Vortex Ring Formation. *J. Fluid Mech.*, 1998, **360**, 121-140.
- [17] G. Peng, S. Shimizu and S. Fujikawa. A Numerical Study of Turbulent Vortex Cavitating Flows in a Submerged Water Jet (in Japanese). *J. Jet Flow Eng.*, 2008, **25(2)**, 11-17.
- [18] K. Nakano, M. Hayakawa and S. Fujikawa. Observation of Cavitation bubbles in a Starting Submerged Water Jet (in Japanese). *Trans. JSME (B)*, 2003, **69**, 360-367.